Evaluation of Non Conservatism of Combined Rainflow Counting and Miner's Rule for Damage Cumulation in Strain Controlled Fatigue

Taheri Said[1] *and Doquet Veronique*[2]

(1) Division R &D, Electricité de France 1. Av. Général de Gaulle Clamart 92141 Cedex France
(2) Laboratoire de mécanique des solides, Ecole Polytechnique-CNRS, 91128 Palaiseau Cedex *France*

ABSTRACT

One of the aims of this paper is to show the difference between strain and stress control in uniaxial and non proportional constant amplitude loading and in uniaxial variable amplitude loading. An experimental program has been realised on two stainless steel 304L and 316L and a ferritic A42 steel. For uniaxial constant amplitude loading we show that for 316L and 304L stainless steel, cyclic overloading has a positive effect on lifetime in stress control and a negative effect in strain control, while these effects are negligible for the ferritic steel. Tests performed on 316 stainless steel show that stress controlled constant amplitude out of phase tension-torsion loadings are less damaging than uniaxial equivalent ones, in contrast with strain controlled tests.

In variable amplitude loading we show that a rainflow counting procedure combined to Miner's damage cumulation rule is conservative for stress controlled tests but not for strain controlled tests.

For uniaxial constant amplitude loading a new linear damage cumulation rule is proposed. It takes into account the memory effect in terms of cyclic behaviour and is in accordance with experimental results. Moreover a conservative damage cumulation is proposed for the case of strain control. The modelling is extended to the case of non proportional loading and agrees with experimental data.

An attempt has been done to extend this model to the case of variable amplitude loading but the results are not conclusive.

INTRODUCTION

More than fifteen leak events caused by thermal fatigue cracking of PWR reactor coolant piping have been reported in the world. For the French power plants thermal fatigue appears on some elbows made of 304L stainless steel as thermal crazing. To have a fine analysis of the thermal fatigue problem under variable amplitude loading ; rainflow counting associated with Miner's rule is usually used. Even though this method of damage cumulation gives satisfactory results in car and aeronautical industry, it may require complementary validation for nuclear plant structures.

The problem may be stated as follows : rainflow counting generally overestimates loading amplitudes; moreover in stress controlled tests overloading is beneficial to the fatigue life. Therefore, in car and aeronautical industry, as the loading is usually a stress control one (weight & pressure), combining rainflow counting and the Miner rule usually gives a conservative estimate of damage. However, for thermal loading, the local loading is generally strain controlled and an overload reduces the fatigue life. In some cases, the overestimation of loading amplitudes by the rainflow counting method may not be sufficient to compensate the reduction of endurance due to overloading so that a non conservative estimation of damage may be obtained.

In the following, experimental results concerning the influence of a few cyclic overloads on the fatigue life of 304L and 316L stainless steels and A42 mild steel during stress or strain controlled push-pull tests are presented. Results concerning the fatigue life of 316L stainless steel in either stress or strain controlled biaxial non proportional loading are compared. Variable amplitude push-pull tests performed in stress or strain control on 304L stainless steel are finally described.

A linear damage cumulation method taking into account memory effects in terms of cyclic behaviour is presented [1,2] and the previsions of fatigue lives issued from this model are compared to experimental results and to the previsions obtained by rainflow counting associated with Miner's damage cumulation rule.

EXPERIMENTS

Uniaxial constant amplitude loading

Push-pull tests were performed on cylindrical specimens of A42 mild steel, 304L and 316L stainless teels, in strain control, for the first two materials and in stress control for the later.

The cyclic behaviour and the endurance of A42 mild steel in the as received condition as well as after 10 cycles at a strain range of ±1.85% were compared [3]. It appeared that the memory of the prestrain is lost at steady-state and that the overload cycles do not have a significant effect on the fatigue life (figures 1-a and 1-b).

By contrast, 304L stainless steel submitted to similar prestrain (10 cycles at ±1.9% and return to zero strain by unloading from peak tensile or peak compressive strain) keeps some memory of this prestrain in terms of stress range (Figure 2-a, and table 1) and residual mean stress (figure 2-b). Moreover an important secondary hardening is detected (figure 2-c). This memory effect is associated with a strong reduction in fatigue life, even when a compressive residual stress is present (figure 2-d). Howether, figure 2-e shows that the detrimental effect of the prestrain is not as high as one could infer from the introduction of the stress-range measured for the prestrained material in Wöhler's curve of the annealed steel. Figure 2-f shows the steady state for the virgin metal at ±0.226% . It may noted that even for high cycle fatigue (more than 10^6 cycles) cyclic plasticity is non negligible.

The cyclic behaviour and endurance of 316L stainless steel was characterised by stress controlled push-pull tests performed after 50 cycles at $\pm 370 MPa$ or 30 cycles at $\pm 423 MPa$ or on the annealed material. (The number of overload cycles is low enough to avoid crack initiation). Figure 3a shows that the material keeps some memory of the prestress (so that the pastic strain range is smaller than for the virgin material for a similar stress range). It can be seen on figure 3b that these overload cycles have a slightly beneficial influence on the fatigue life.

Biaxial constant amplitude non proportional loading.

90° out of phase tension and torsion tests were performed on tubular specimens of 316L stainless steel (12.5mm outer diameter, 1.25mm wall thickness, 20mm gage length) equipped with a biaxial extensometer. The results of these tests are compared with uniaxial data on Figures 3a and 3b. It appears that non proportional loading, known for its strongly detrimental influence on the fatigue life of 316 stainless steel, in strain control [4] has a beneficial influence, in stress control.

Uniaxial variable amplitude loading

Three variable amplitude push-pull tests have been performed on 304L stainless steel in stress control, following loading paths derived from a signal of 1825 cycles obtained on an elbow mock-up of an auxiliary cooling system in a French PWR plant. To get different amplitudes and different mean stresses this signal was amplified by various factors (positive or negative but larger than one in absolute value in order to keep test durations reasonable). As the endurance limit does not seem to have a clear meaning for variable amplitude loading, different *thresholds* on loading amplitudes were used below which the cycle was eliminated.

Table 2 specifies the amplification factors and the thresholds used to define the loading path applied during the tests. It gives also the mean stress and the observed fatigue lives (number of repeated blocs at fracture times the number of extracted cycles). Figures 4a to d concern the stress controlled test number 1 and show respectively, the applied stress signal, the strain response at midlife, the evolution of the strain amplitude and of the mean strain with the number of bloc repetition. A substantial ratchetting effect due to the positive mean stress is observed.

It is not straightforward to define a *strain loading path « equivalent » to a stress controlled loading* without doing any elastoplastic simulation. One simple way to do this is to take for each successive peak value of the stress loading path the corresponding strain value on the tensile or cyclic stress-strain curve. This method was applied for each of the three stress controlled tests presented above (after amplification), using the cyclic plastic-strain/stress curve, and considering the derived pastic strain as a total strain. The damage produced by the strain loading path calculated that way should thus be less than the damage obtained if the « equivalence » had been done using the cyclic total-strain/stress curve. (The cyclic curve was extrapolated by symetry for the case of compressive peak stresses). In tests 1 and 2 the threshold on the strain range was smaller than the one which is « equivalent » to the threshold on the stress range through the cyclic stress-strain curve. That means that smaller cycles will be preserved in strain controlled test. This should lead to a higher fatigue life (since they do contribute to the number of cycles in a bloc). Figures 5a and 5b show respectively the imposed strain path and the measured evolution of the mean stress with the number of bloc repetion for the strain controlled test number 1 (deduced from the stress loading number 1 by the procedure described above).

An additional test (number 3bis) was performed, applying the amplification factor to the « equivalent » strain path and not to the original stress path.The results of the four strain controlled tests are presented in Table 2 where the mean stress at steady state is also specified. It appears that a strain path obtained through the « equivalence » procedure after amplification is more damaging than a srain path amplified after the « equivalence » procedure (compare strain controlled tests number 3 and 3bis). This is due to the decreasing slope of the cyclic stress-strain curve (in the first case, the maximal stress is also amplified and for a given stress range, the corresponding strain range will be larger, the larger the maximal stress is), see figure 6.

MODELLING

Uniaxial constant amplitude loading.

Figure 7 shows the cyclic stress-strain curves for 316L steel obtained through strain controlled push-pull tests. Curve A is the curve obtained by increasing the amplitude stepwise. Curve B is the curve obtained by decreasing the strain range from point H to N. Curve C is the curve obtained by increasing the amplitude from point N. Curve B demonstrates that the memory of high amplitudes is preserved for low amplitudes. These curves will be used to explain the sequence effect. Here we consider two type of loading : a Low-High (L-H) sequence and a High-Low (H-L) sequence.

In *strain control*, for a L-H sequence, stabilisation for load L corresponds to point L_1 and for load H, to point H. So the cumulated damage is :

$$D^{\varepsilon}_{L-H} = n_L / N_f\left(\Delta\varepsilon_L\right) + n_H / N_f\left(\Delta\varepsilon_H\right) \quad (1)$$

n_L and n_H denote the number of applied cycles, and $N_f\left(\Delta\varepsilon_L\right)$ and $N_f\left(\Delta\varepsilon_H\right)$ denote the fatigue lives under low and high amplitude respectively. D^{ε} means that the computing uses a Manson-Coffin curve. If we apply a H-L sequence, the stabilization points will be H and L_2 (transient cycles having been disregarded for the damage cumulation). The cumulated damage for the H-L sequence is larger than for the L-H sequence, since the stress amplitude is greater at point L_2 than at point L_1, for identical strain amplitudes. Fatigue curves with cyclic overloading being scarce in the literature, to obtain a conservative prediction we replace the point L_2 by L_4. We take then as cumulated damage the conservative value :

$$D^{\varepsilon}_{H-L} = n_L / N_f\left(\Delta\varepsilon_{L_4}\right) + n_H / N_f\left(\Delta\varepsilon_H\right) \quad (2)$$

For 316 stainless steel in low cycle fatigue the fatigue lives estimated by the previous model, were compared succesfully to experimental data in reference [1]. For the present data obtained on 304L steel the previsions of this conservative model are presented in Table 1.

In *stress control*, the L-H sequence gives points L_1 and H and the H-L sequence gives points H and L_3. Contrary to the previous case, the cumulated damage for the H-L sequence is smaller than for the L-H sequence, since the strain amplitude is greater at point L_1 than at point L_3, for identical stress amplitude. This is confirmed by experimental data presented on figure 3b. In stress control, a conservative estimate of damage may thus be obtained neglecting the overloads.

Biaxial non proportional loading

For damage cumulation in non proportional situations, an equivalence [1,2] is proposed between a cyclically non proportional steady state and a uniaxial steady state with cyclic prehardening : the non proportional steady state defined by $(\Delta\varepsilon_{eq}, \Delta\sigma_{eq})$ corresponding to point L_3 in Figure 1, is considered to be equivalent to a steady state obtained by $\Delta\varepsilon_{11} = \Delta\varepsilon_{eq}$ (strain-controlled) or $\Delta\sigma_{11} = \Delta\sigma_{eq}$ (stress-controlled) after cyclic overloading up to stabilisation at point H. Through this the previous experimental data (figures 3a and 3b) may be explained : in stress control damaging is less than uniaxial equivalent one in contrast with strain control tests. Moreover a conservative damage cumulation for the case of non proportional strain control is proposed by replacing point L_3 by L_1.

Uniaxial variable amplitude loading (rainflow counting + Miner's rule)

For the simulations, rainflow counting combined to the linear damage cumulation rule is used. The fatigue curve is the one presented in the figure 2d, where a linear extrapolation for high number of cycles is used. This means that small cycles below the apparent endurance limit (figure 2d) which have not been eliminated through threshold contribute to damage in the simulations, while we do not know if it is the case for the experiments. However this should make the analysis conservative. For the case of positive mean stress a Goodman correction has been used through the multiplication of the loading range by $\alpha = 1 + (\sigma_m / \sigma_u)$, where σ_m is the measured mean stress at steady-state and σ_u is the ultimate stress which has been taken equal to 540 MPa. The estimations of the fatigue lives by this method are reported in table 2. They are conservative for stress controlled tests but seriously non conservative for strain controlled tests.

Uniaxial variable amplitude loading

The estimations of the fatigue lives issued from the proposed model are presented in table 2 for strain controlled tests. The predictions are not conservative here, contrary to constant amplitude loading, even though they are more pessimistic than rainflow counting associated with Miner's rule for strain controlled tests number 1 and 2. For strain controlled test number 3

the prediction is even less conservative than rainflow counting + Miner's rule. This is because rainflow counting overestimates the loading ranges, which is not the case for natural counting used in the proposed model. In this case this overestimation of the amplitudes by rainflow counting is larger than the overestimation of damage proposed by our model (replacing L_1 by L_4 figure 7).

CONCLUSIONS

A linear damage cumulation method taking into account memory effects in terms of cyclic behaviour was presented and its previsions compared to experimental data obtained on one ferritic and two austenitic stainless steels. The model conservatively predicts the life reduction due to a few cyclic overloads or to biaxial non proportional loading in strain controlled tests performed on stainless steels. Consistent with experiments, it also predicts that in stress control, neither cyclic overloading nor biaxial non proportional loading are detrimental and that the fatigue life of a ferrictic steel which does not keep any memory of prestrain is not significantly affected by cyclic overloading.

Variable amplitude push-pull tests have shown that under stress control, rainflow counting method combined to Miner's damage cumulation rule yield conservative damage estimates, provided the influence of the mean stress is taken into account through Goodman's correction, while for strain control, the estimations may not be conservative. For those cases, the proposed model does not succeed either and will have to be improved.

REFERENCES

1. Taheri,S., (1996) Multiaxial and fatigue design, MEP Publications, Elsevier, London, p 283.
2. Taheri S. Doquet V. (1998) Lifetime management and evaluation of plant, structures and components, AEA congress, Cambridge, GB, p-59.
3. Doquet V.and Taheri S., (2000), Revue Française de mécanique n° 2000-1.
4. Doquet,V. and Pineau,A., (1990), Scripta Met. Mater., Vol. 24, p433.

TALE 1 : Strain controlled, constant amplitude loading

Cyclic TESTS, Metal as recieved				**MODELLING**	
$\Delta\varepsilon^p/2$	$\Delta\Sigma/2$	N_f		$\Delta\varepsilon^p/2$	N_f
1,10E-03	226	> 5821297		6,00E-04	23700
1,16E-03	228	> 4676289		9,80E-04	21600
1,55E-03	230	2,39E+05		1,67E-03	15900
1,41E-03	231	1,50E+05		3,74E-03	2200
1,66E-03	239	7,35E+04		6,00E-03	600
1,99E-03	270	3,38E+04			
4,00E-03	341	2,85E+03			
6,12E-03	394	1,07E+03			
7,00E-03	421	5,62E+02			
Cyclic TESTS, Metal prehardened cyclically at +/-1.9%					
$\Delta\varepsilon^p/2$, $\Sigma m>0$	$\Delta\Sigma/2$, $\Sigma m>0$	N_f , $\Sigma m>0$	$\Delta\varepsilon^p/2$, $\Sigma m<0$	$\Delta\Sigma/2$, $\Sigma m<0$	N_f $\Sigma m<0$
1,50E-04	261	165229	1,50E-04	3,10E+02	> 5240000
3,30E-04	301	98910	1,65E-04	2,78E+02	> 4029102
6,00E-04	293	37247	1,50E-04	2,62E+02	602128
9,00E-04	288	48870			
9,80E-04	298	13221			
1,67E-03	311	16250	$\Delta\varepsilon^p/2$, $\Sigma m=0$	$\Delta\Sigma/2$, $\Sigma m=0$	N_f, $\Sigma m=0$
3,74E-03	360	1854	6,50E-04	283	139143
6,02E-03	417	865	8,80E-04	293	47745

TALE 2 : stress and strain controlled variable amplitude loading

LOADING TYPE	**stress** (1)	**strain**(1)	**stress**(2)	**strain**(2)	**stress**(3)	**strain**(3)	**strain** (3bis)
number of cycles in the initial bloc loading	1825	1825	1825	1825	1825	1825	1825
amplification factor	- 4	+ 4	+3.6	+3.6	-3.3	-3.3	-3.3
thresholds in $\Delta\sigma$, and $\Delta\varepsilon$ for the tests	360 MPa	0,0286 %	324 MPa	0,0338 %	328 MPa	0,0814 %	0,0814 %
number of cycles in a bloc after extraction	76 rainflow	668 rainflow	76 rainflow	571 rainflow	76 natural	295 natural	76 natural
mesured mean stress at steady state (last bloc)	+ 54 MPa		- 49 MPa		+53 MPa		
maximal mean stress on the respone (last bloc)		- 20 MPa		+ 120 MPa		- 160 MPa	- 145MPa
FATIGUE LIVES number of cycles							
Experimental	**80 000**	**37 000**	**588 000**	**69 000**	**450 000**	**413 000**	**2244 000**
Rainflow + Miner	**77 000**	**92 000**	**263 000**	**592 000**	**580 000**	**1063 000**	**2286 000**
Rainflow + Miner + Goodman correction	**29 000**			**213 000**	**215 000**		
Proposed modelling		**69 000**		**415 000**		**1360 000**	
Proposed modelling + Goodman correction				**150 000**			

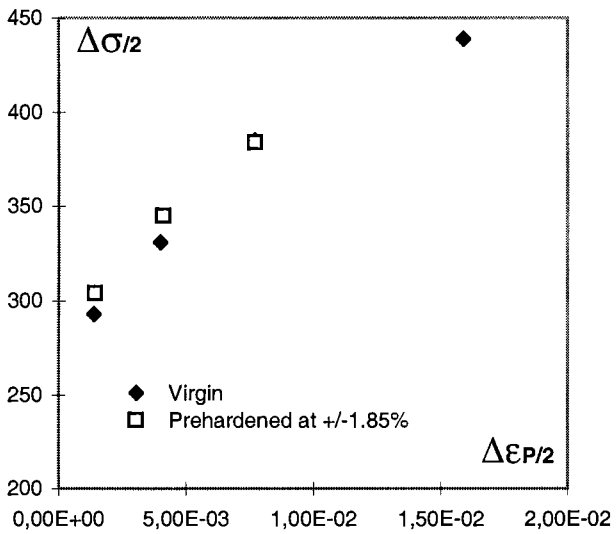

Figure 1a : Cyclic curves without and with cyclic prehardening for a ferritic A42 steel

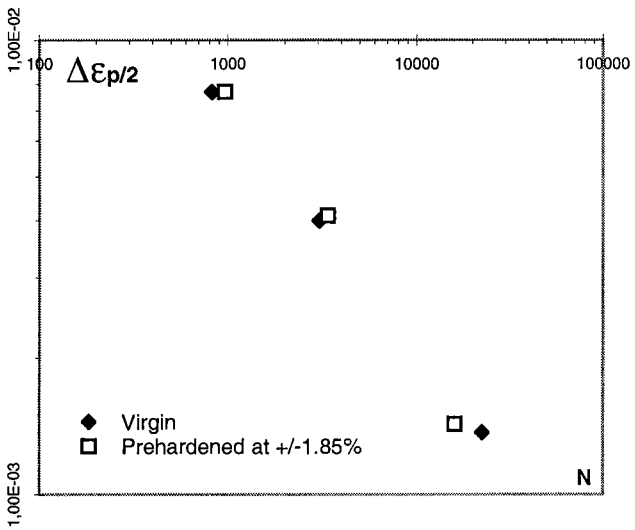

Figure 1a : fatigue curves without and with cyclic prehardening for a ferritic A42 steel

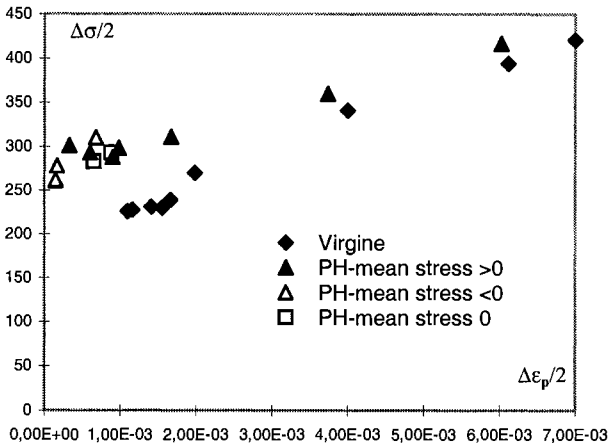

Figure 2-a : cyclic curves for a 304 L steel (PH : prehardened)

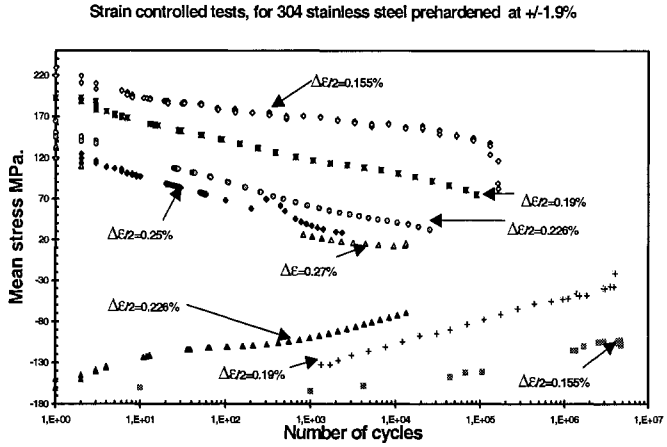

Figure 2-b : Evolution of mean stress in strain controlled tests

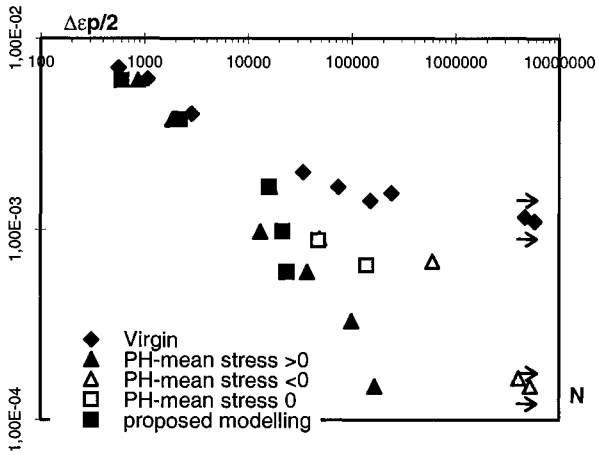

Figure 2-d : fatigue data strain controlled

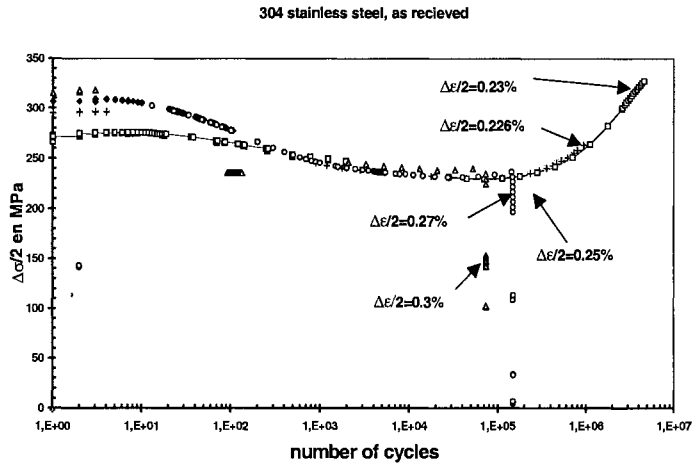

Figure 2-c Secondary hardening at diffrent strain amplitudes

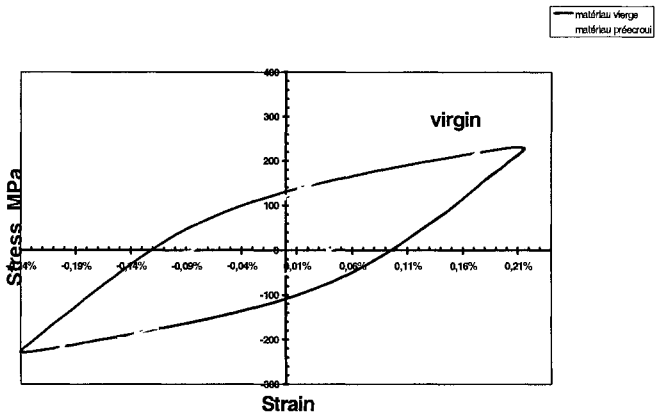

Figure 2-f : Steady state for 304L, strain cycling at +/-226%

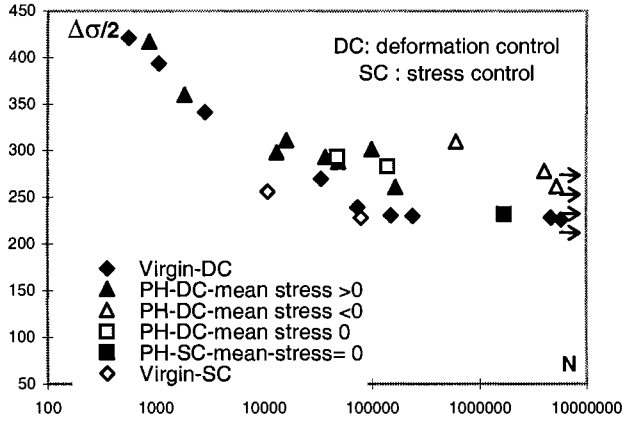

Figure 2-e : fatigue data for 304 L stess and strain controlled (PH : prehardened)

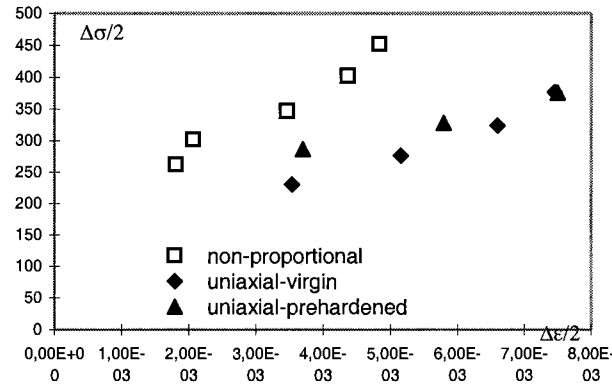

Figure 3-a : stress controlled cyclic curves, 316L steel

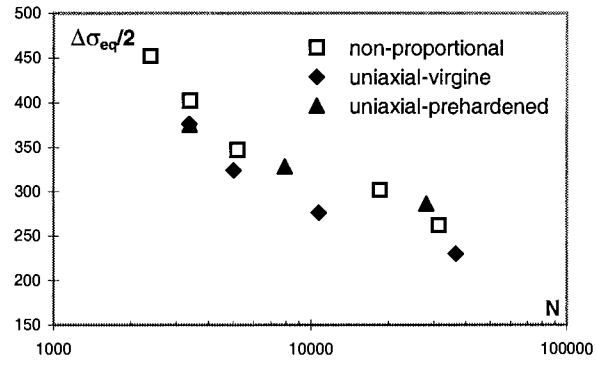

Figure 3-b stress controlled fatigue data, 316 steel

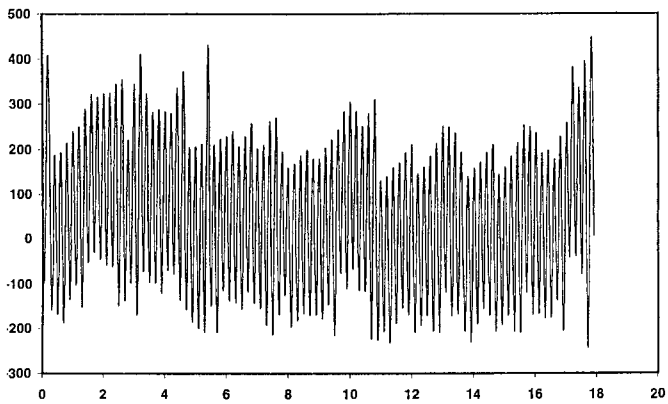

Figure 4-a : extracted stress signal on a bloc loading

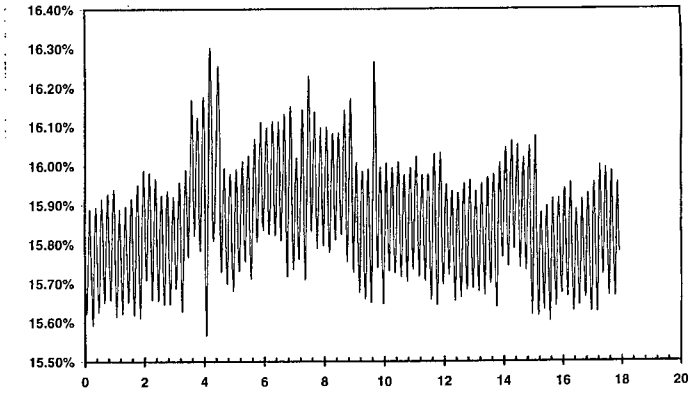

Figure 4-b : strain response at bloc loading number 325

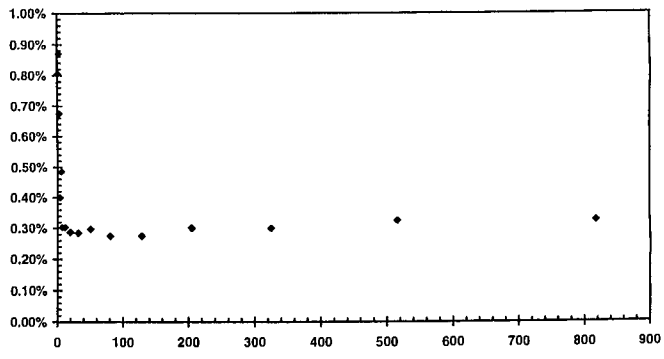

Figure 4-c : amplitude of strain versus number of bloc

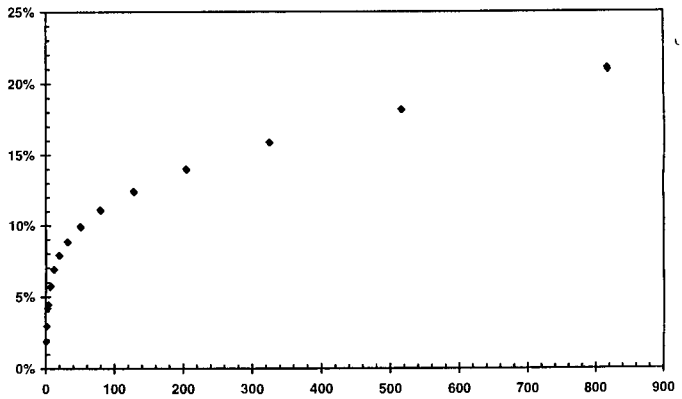

Figure 4-d : mean strain versus number of bloc

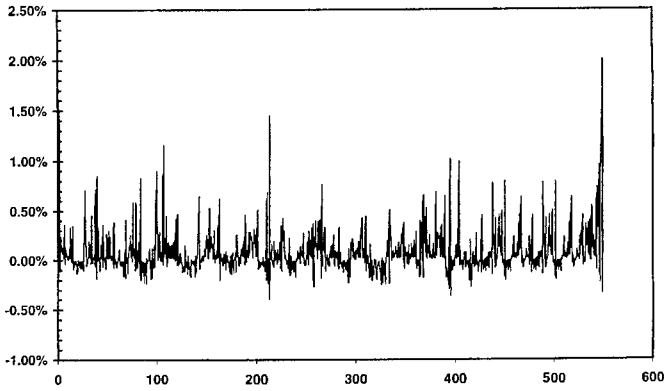

Figure 5-a : equivalent strain loading to stress load figure 4a

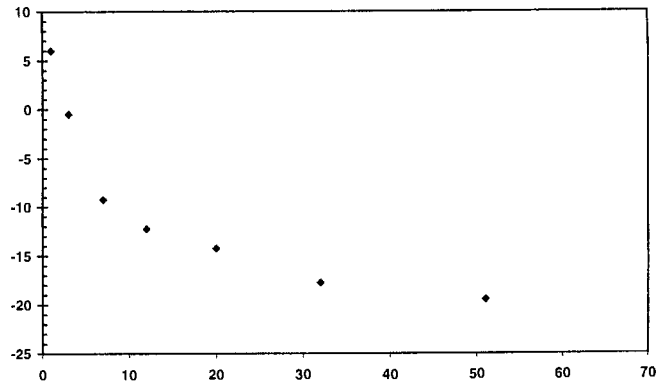

Figure 5-b mean stress versus number of bloc for strain loading

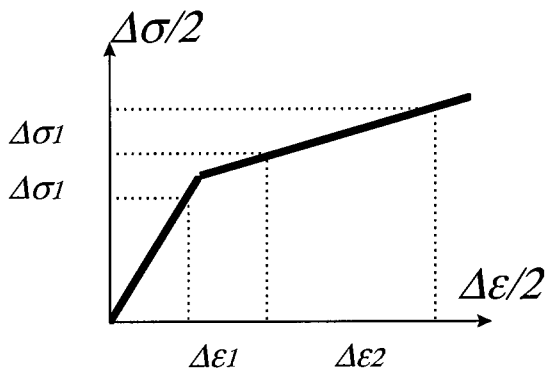

Figure 6 : two strain amplitudes equivalent to the same stress amplitude for differents maximal stresses corresponding to loading 3 ($\Delta\sigma 1, \Delta\varepsilon 1$) and 3bis ($\Delta\sigma 1, \Delta\varepsilon 2$)

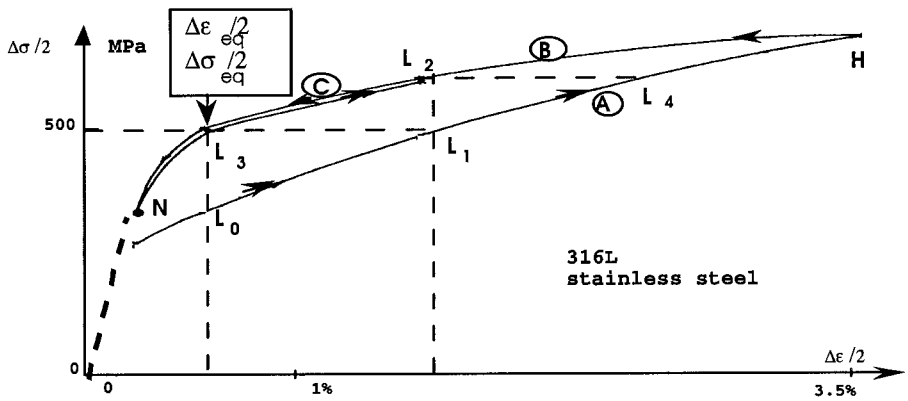

Figure 7 : cyclic curve without and with cyclic prehardening